6

Environmental effects on photoluminescence of single-walled carbon nanotubes

Yutaka Ohno, Shigeo Maruyama* and Takashi Mizutani
Department of Quantum Engineering, Nagoya University
**Department of Mechanical Engineering, The University of Tokyo*
Japan

1. Introduction

Spectroscopy is a powerful technique to characterize single-walled carbon nanotubes (SWNTs). In particular, photoluminescence (PL) and excitation spectroscopies have enabled to make great advances in understanding the energy states and transition processes of excitons in SWNTs. Furthermore, PL spectroscopy also has potential for being used to determine the chiral index (*n*,*m*) of an SWNT and evaluate the abundance of (*n*,*m*) in bulk SWNTs. (Bachilo, Strano et al. 2002; Miyauchi, Chiashi et al. 2004) However, in order to establish PL spectroscopy as a reliable standard technique to characterize SWNTs, it is necessary to understand not only the intrinsic physics of excitons but also the effects of extrinsic factors, namely, *environmental effects*. (Fantini, Jorio et al. 2004) The optical properties of an SWNT are modified sensitively by its environmental conditions because of the excitons existing on the SWNT surface. In this chapter, we focus on the environmental effects on the optical properties of SWNTs. After considering the fundamental physics of the optical transitions in SWNTs and application of PL spectroscopy to characterize SWNTs, various types of environmental effects are discussed with practical examples.

2. Optical transition and photoluminescence

2.1 Density of states and optical transition

In an SWNT, electrons are confined to its surface, and the wave vectors along the circumference are quantized by a periodic boundary condition; however, the carriers are free to move in the direction of the SWNT axis. Therefore, the SWNT has a one-dimensional electron system, where the density of states is characterized by the sharp peaks originating from a van Hove singularity, as shown in Fig. 1(a). (Saito, Dresselhaus et al. 1998)

An optical transition in an SWNT occurs dominantly between two subbands located at van Hove singularities. However, because of the one-dimensional structure, it depends on the polarization of the incident light. If the incident light is polarized linearly with the polarization vector parallel to the SWNT axis, a strong optical transition occurs. In this case, the optical transitions from a subband of a valence band to a subband of the conduction band, and vice versa, with the same quantum number are allowed by the selection rule. For

example, transitions such as those from C1 to V1 and from V2 to C2 are allowed transitions, as shown in Fig. 1(a). On the other hand, if the incident light is polarized perpendicular to the SWNT axis, the optical transition is strongly suppressed by the depolarization effect in which the induced charges cancel the electric field of the light in the SWNT. (Duesberg, Loa et al. 2000)

The energy of an optical transition is given by the difference in the energies of the two subbands, in the case of the single-particle approximation. However, in practice, it is modified by many-body effects, as shown in Fig. 1(b). (Ando 2005) The single-particle bandgap E_{ii}^{gr} is renormalized by the self-energy of an electron due to the repulsive interaction between electrons. In addition, for an optical transition, the exciton effect should be taken into account, that is, the optical transition energy is decreased by the binding energy of the attractive Coulomb interaction between an electron and a hole. In the case of SWNTs, since the exciton binding energy is as large as a few hundred millielectronvolts, the exciton scheme is more suitable than the single-particle scheme. (Wang, Dukovic et al. 2005) Consequently, the optical transition energy E_{ii} between the i-th valence band and the i-th conduction band (i = 1, 2, 3, …) is given by

$$E_{ii} = E_{ii}^{gr} + E_{ii}^{ee} + E_{ii}^{eh}, \quad (1)$$

where E_{ii}^{ee} denotes the energy of repulsive interaction between electrons, and E_{ii}^{eh} (< 0) represents the binding energy of an exciton. Note that every term is perturbed by the environment around the SWNT, as described later.

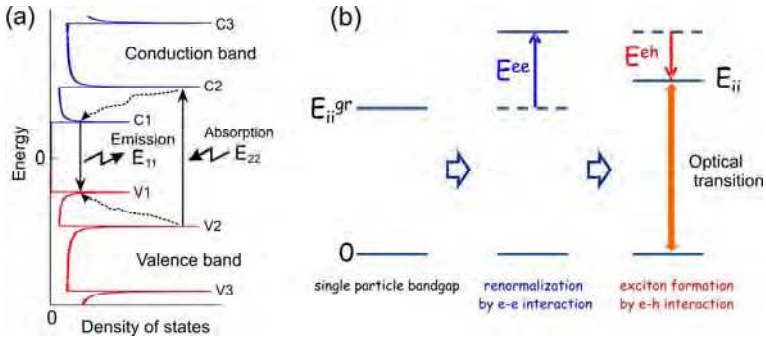

Fig. 1. (a) Density of states of a semiconducting SWNT and optical transition processes in the single particle scheme. (b) Energy diagram of an exciton state, showing optical transition energy in the exciton scheme.

2.2 Photoluminescence spectroscopy

Since the optical transition energy E_{ii} depends on the chiral index (n,m) of an SWNT, (n,m) can be determined by spectroscopic techniques such as Raman scattering spectroscopy (Kataura, Kumazawa et al. 1999) and photoluminescence (PL) spectroscopy. (Bachilo, Strano et al. 2002) In the case of PL spectroscopy of a semiconducting SWNT, the E_{22} state is resonantly excited by incident light so as to generate excitons, as shown in Fig. 1(a). (O'Connell, Bachilo et al. 2002) The excitons relax via phonons to the E_{11} state, where

radiative recombination occurs. Figure 2(a) shows the PL spectra of SWNTs measured at various excitation wavelengths. Such measurement is called the PL mapping measurement. Each peak originates from a different (n,m) species. From the relative intensity of each peak, the abundance of each (n,m) species can be evaluated. It should be note that the quantum efficiency of light absorption and emission depends on the diameter and chirality of SWNTs. (Oyama, Saito et al. 2006) Therefore, in order to make accurate evaluation of the (n,m) abundance, a correction of the (n,m) dependence of the quantum efficiency is required. (Okazaki, Saito et al. 2006)

Figure 2(b) shows the E_{22} vs. E_{11} plot for various (n,m) species, which are derived from the PL map of Fig. 2(a). The points connected by a solid line belong to the family of SWNTs that have the same value of ($2n + m$). (Saito, Dresselhaus et al. 1998) It can be observed that the family patterns are separated into two groups, depending on the value of ($2n + m$ mod 3). In this chapter, we define these two groups as Type I if ($2n + m$ mod 3) = 1, and Type II if ($2n + m$ mod 3) = 2. When a graphite layer is rolled up to form an SWNT, the quantized energies of the subbands primarily depend on the diameter of the SWNT. In addition, they also depend on the direction to be quantized, namely the chiral angle, because the equi-energy contours of graphite are warped to form a triangular shape around the K point, which is called the trigonal warping effect. (Saito, Dresselhaus et al. 2000) This is the main reason for the appearance of the family pattern in the plot of optical transition energies.

The family patterns are technically important for the analysis of PL spectra. Even though the optical transition energies of SWNTs vary by more than 100 meV, depending on the methods used to prepare SWNTs and on the environment, the identification of the family pattern allows us to easily determine the chirality index (n,m) of the SWNTs.

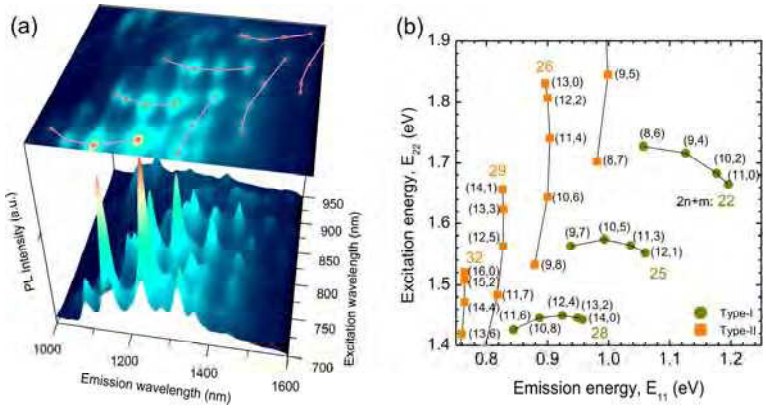

Fig. 2. (a) PL spectra of SWNTs measured for various excitation wavelengths (PL map). (b) E_{22} vs. E_{11} plot. A solid line connects SWNTs belonging to the same family, i.e., SWNTs having the same value of $2n + m$.

2.3 Relaxation process

In PL processes, the excitons excited to the E_{22} state relax to the lowest state E_{11} via phonons in a short time such as ~0.1 ps because the optical phonon energy is as large as 0.2 eV (Ichida, Hamanaka et al. 2002; Ostojic, Zaric et al. 2004) Then, the excitons relax to the ground state

via radiative recombination or nonradiative recombination. The radiative recombination lifetime is expected to be about 1 ns. (Spataru, Ismail-Beigi et al. 2005) In contrast, the experimental results of pump-probe measurements and time-resolved PL measurements have shown a much shorter recombination lifetime, of the order of several tens of picoseconds. (Hagen, Moos et al. 2004; Wang, Dukovic et al. 2004; Hirori, Matsuda et al. 2006; Ohno, Kishimoto et al. 2006) Such a short recombination lifetime suggests that the dominant recombination process is nonradiative. The luminescence quantum efficiency has been estimated experimentally to be several percent. (Lefebvre, Austing et al. 2006) Recombination centers formed by defects and interface states may enhance such nonradiative recombination. It has been suggested that nonradiative recombination rate is enhanced if the exciton is localized. (Perebeinos and Avouris 2008)

2.4 Sample preparation for achieving photoluminescence

The soot of SWNTs generally consists of SWNT bundles formed by van der Waals interaction. In a bundle of SWNTs, the energy of photoexcited excitons is transferred to neighboring metallic SWNTs or SWNTs with a smaller bandgap, and then, these excitons relax via phonons. Therefore, in order to obtain luminescence from SWNTs, it is necessary to debundle and individualize SWNTs from a bundle. The PL from individual SWNTs has been observed for the first time by O'Connell et al. by wrapping SWNTs with a surfactant such as sodium-dodecyl-sulfate (SDS) in order to form micelles encasing individual SWNTs. (O'Connell, Bachilo et al. 2002) After dispersing the soot of SWNTs in an aqueous solution of SDS by performing ultrasonication, they obtained individualized SWNTs in the supernatant liquid of ultracentrifugation, as shown in Fig. 3(a).

Another method to obtain individualized SWNTs is to grow SWNTs directly between pillars or on trenches formed on a Si or quartz substrate, as shown in Fig. 3(b). (Lefebvre, Fraser et al. 2004; Ohno, Iwasaki et al. 2006) The free-standing SWNTs bridging such a microstructure provide strong PL, although the PL is suppressed if an SWNT touches the substrate, as will be described later. Further, the PL signal from a free-standing SWNT is sufficiently strong and can hence be observed by a microscopic PL technique.

For the purpose of studying the environmental effects on the PL of SWNTs, free-standing SWNTs grown between pillars or on trenches are suitable because the environmental conditions can be intentionally changed by exposing the SWNTs to a gas (Finnie, Homma et al. 2005; Chiashi, Watanabe et al. 2008) or by immersing the SWNTs in a liquid. (Iwasaki, Ohno et al. 2007; Ohno, Iwasaki et al. 2007)

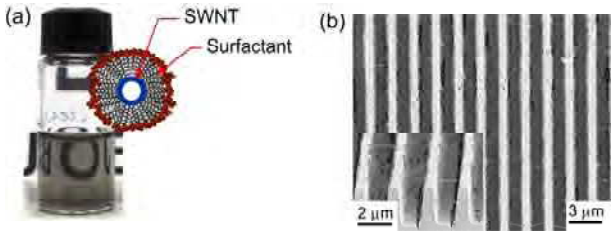

Fig. 3. (a) Photograph of SWNTs dispersed in surfactant solution. (b) SEM image of free-standing SWNTs grown on the trenches formed on a quartz substrate.

3. Environmental effects

The environmental effects on the PL of SWNTs is one of the most important topics as regards the optical properties of SWNTs. (Moore, Strano et al. 2003; Chou, Ribeiro et al. 2004; Fantini, Jorio et al. 2004) It is known that the optical transition energy varies, depending on the type of surfactants used to individualize SWNTs. Lefebvre et al. have also reported that the optical transition energies of SWNTs bridging micropillars show a blueshift as compared to the SDS-wrapped SWNTs. (Lefebvre, Fraser et al. 2004) A later study by Ohno et al. has shown that the energy differences depend on (n,m), particularly on the chiral angle and the type of SWNTs, i.e., whether the SWNTs are of Type I or Type II. (Ohno, Iwasaki et al. 2006) One of the causes of the variation in the optical transition energy is the dielectric screening of the many-body interactions between carriers. (Perebeinos, Tersoff et al. 2004; Ando 2005) In addition to the dielectric screening effect, various environmental factors such as chemical interactions (Finnie, Homma et al. 2005; Hertel, Hagen et al. 2005) and mechanical interactions (Arnold, Lebedkin et al. 2004) should be considered. Comprehensive understanding of the environmental effects is necessary to understand the optical properties of SWNTs. In this section, we discuss the effects of the following factors on the PL of SWNTs: dielectric screening, wrapping SWNTs with surfactants, exposing SWNTs to air, doping SWNTs with carriers, and allowing SWNTs to make contact with a substrate.

3.1 Dielectric screening effect

The variation in the optical transition energy caused by the environmental conditions is primarily due to the dielectric screening effect, whereby the many-body Coulomb interactions between carriers are screened by the surrounding material. As shown in Fig. 4, the electric force lines contributing to the Coulomb interactions pass through not only the inside of an SWNT but also the outside, where the surrounding material screens the electric force lines depending on its dielectric constant.

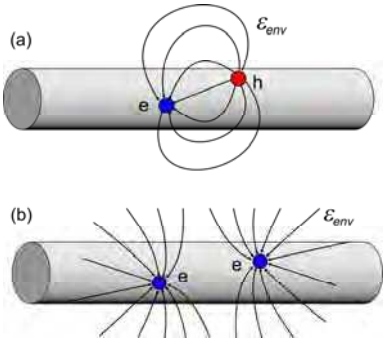

Fig. 4. Schematics of electric force lines contributing to many-body Coulomb interactions: (a) electron-hole attractive interaction, which forms an exciton, and (b) electron-electron repulsive interaction.

Ohno et al. have studied the dielectric screening effect in detail by immersing the SWNTs grown on trenches (Fig. 3(b)) in various organic solvents with dielectric constants from 1.9

to 37. (Iwasaki, Ohno et al. 2007; Ohno, Iwasaki et al. 2007) Figure 5 shows the typical PL spectra measured in the ambient air, hexane (dielectric constant: 1.9), chloroform (4.8), and acetonitrile (37). Note that although in this chapter, the dielectric constants are used considering a dc field, they depend on the frequency of the field. At the frequency corresponding to the exciton lifetime, a dielectric constant is expected to approach unity. Further, although the exact values of ac dielectric constants of these liquids have not been known, they could be related to the dc dielectric constants. The peaks exhibit a redshift and broadening with the increasing dielectric constant of liquids. As indicated by the E_{22} vs. E_{11} plots shown in Fig. 6, both E_{11} and E_{22} exhibit a redshift with the increasing dielectric constant of liquids, with a small (n,m) dependence. The amounts of the redshifts are 20~43 meV for E_{11} and 15~33 meV for E_{22}.

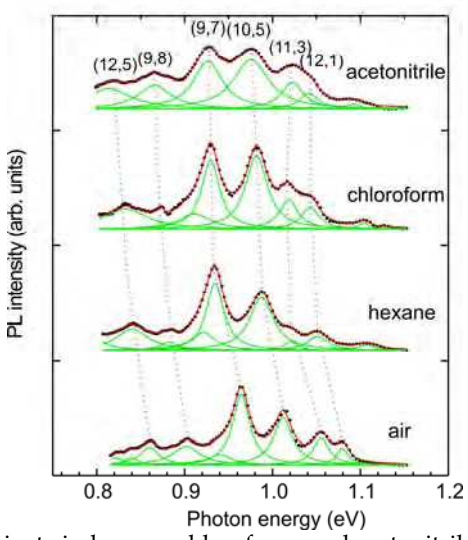

Fig. 5. PL spectra in ambient air, hexane, chloroform, and acetonitrile.

As the dielectric constant increases, the energies of both the electron-electron and electron-hole interactions decrease. The reduction in the exciton binding energy causes a blueshift in the optical transition energy because of the negative energy, whereas the reduction in the electron-electron repulsion energy causes a redshift. The occurrence of redshifts suggests that the variation in the electron-electron repulsion energy is larger than that in the exciton binding energy. This is due to the fact that the repulsion energy is larger in magnitude than the exciton binding energy. (Ando 2005; Spataru, Ismail-Beigi et al. 2005)
Figure 7 shows E_{11} and E_{22} of (8,6)-SWNTs as a function of the dielectric constant of the surrounding liquid. The energy shift is significant in the regime of a low dielectric constant, and exhibits a tendency to saturate at a dielectric constant of ~5. Empirically, the dependence of E_{ii} on the environmental dielectric constant ε_{env} is given by

$$E_{ii} = E_{ii}^{\infty} + A\varepsilon_{env}^{-\alpha}. \quad (2)$$

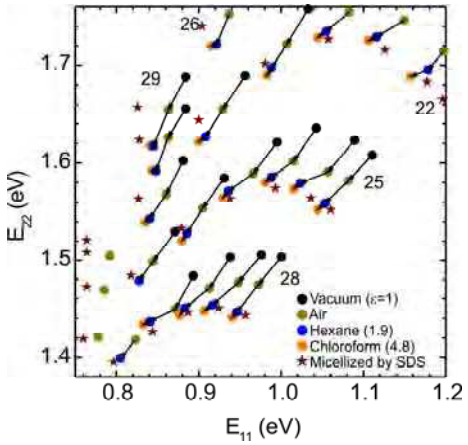

Fig. 6. E_{22} vs. E_{11} plots of SWNTs grown on microtrenches in various environmental conditions: in vacuum (black dots), air (yellow green), hexane (blue), chloroform (orange), and aqueous solution of SDS (red stars).

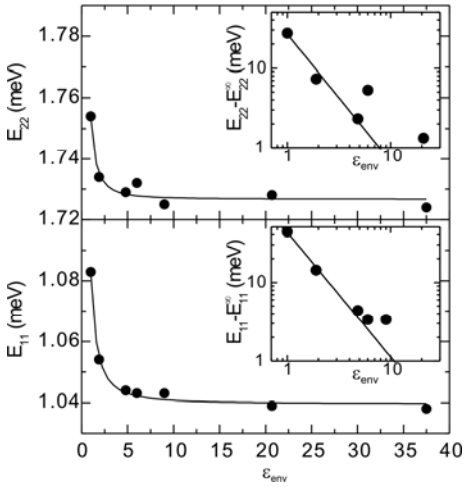

Fig. 7. E_{11} and E_{22} of (8,6)-SWNTs as a function of the dielectric constant of the surrounding liquid. The insets are the log-log plots.

In Eq. (2), the first term on the right-hand side corresponds to the transition energy when ε_{env} is infinity; it consists of the single-particle bandgap and the energies of the many-body interactions, which are determined by the electric force lines traveling only inside the SWNT. The second term shows the screening of Coulomb interactions, including both electron-hole binding and electron-electron repulsive interactions, which are related to the electric force lines traveling outside the SWNT. In the equation, "A" denotes the maximum energy variation. In Fig. 6, the solid curves are fitted to the data by using Eq. (2). Here, A and α are 43 meV and 1.6 for E_{11}, and 27 meV and 1.8 for E_{22}, respectively. Miyauchi et al. have also

obtained a power-law-like dependence of the exciton transition energies on the dielectric constant of the material surrounding SWNTs by the tight-binding calculation.(Miyauchi, Saito et al. 2007)
The variation in E_{ii} due to the dielectric screening effect also depends on (n,m), particularly, on the chiral angle, and the type (Type I or Type II). This may be due to the (n,m) dependence of the effective mass of carriers. As descried before, the effective mass depends on the chiral angle because of the trigonal warping effect. (Jorio, Fantini et al. 2005) In addition, the effective mass is one of the scaling parameters for exciton energy. (Perebeinos, Tersoff et al. 2004) Similarly, the repulsive energy of electron-electron interaction could depend on the effective mass.
It should be noted that in addition to exhibiting the redshift, the PL spectrum became broader when the SWNTs were immersed in liquids with a large dielectric constant, as shown in Fig. 5. The full width at half maximum (FWHM) increased from 23 meV in the ambient air to 40 meV in acetonitrile for (9,7)-SWNTs. This linewidth broadening may be attributed to inhomogeneous broadening due to the fluctuation in the local dielectric constant of the environment occurring on the scale of the size of a liquid molecule. It should be mentioned that the dielectric constants used in this chapter are macroscopic and static values. In practice, the size of a molecule of an organic solvent is comparable to that of an exciton; therefore, the local dielectric constant around an exciton could fluctuate depending on the position and orientation of the surrounding organic molecules, which could not follow the dynamic electric field formed by the exciton within the lifetime of the exciton. This results in the dispersion of the energies of many–body interactions.

3.2 Effect of ambient air and intrinsic transition energies

On measuring the PL of free-standing SWNTs in a vacuum, it is found that the transition energies are 20~40 meV higher than those corresponding to the PL measured in the ambient air, as shown by the black dots in Fig. 6. Further, sequential measurements of the PL in the ambient air after the growth of SWNTs exhibit a phenomenon that every E_{ii} shifts to a lower energy with an incubation time ranging from a few hours to several days. The incubation time required for the occurrence of a redshift depends on the diameter of SWNTs, that is, the redshift occurs earlier in the case of SWNTs with a small diameter than that in the case of SWNTs with a large diameter. This variation in E_{ii} is reversible, namely, E_{ii} returns to its former value when the sample is heated up above 50°C in a vacuum. The shifts in E_{ii} can be attributed to the dielectric screening effect because their behavior is similar to that observed in the liquid immersion experiments.
In air, the ambient molecules such as H_2O and C_xH_y are adsorbed on the surface of SWNTs and cause the screening of many-body interactions. Chiashi et al. have investigated the effect of gas adsorption in detail. (Chiashi, Watanabe et al. 2008) They have shown that a redshift occurs at a gas pressure exceeding the transition pressure, which agrees with Langmuir's adsorption model.
Carrier doping due to oxygen molecules should be discussed as one of the effects of the ambient air because the energies of many-body interactions may be modified depending on the carrier density. The effect of carrier doping performed by the field-effect doping technique has been studied by measuring the PL of a free-standing SWNT placed in a field-effect transistor structure. (Ohno, Kishimoto et al. 2006) In addition, the effect of chemical doping with F_4TCNQ (tetrafluorotetracyano-p-quinodimethane), which is a strong *p*-type

dopant for SWNTs (Nosho, Ohno et al. 2007), has also been studied. Even though the carrier densities introduced by these doping techniques were as high as that introduced by the ambient oxygen, the optical transition energies were not significantly modified by doping. This may be because the doping density was probably not sufficiently high to dope carriers in the range of the exciton diameter.
Now, by heating the free-standing SWNTs in a vacuum, the adsorbed molecules can be desorbed, and then the *intrinsic* transition energies of SWNTs can be measured without any environmental effects.

3.3 Effect of wrapping with surfactants

When the free-standing SWNTs grown on trenches were immersed in an aqueous solution of SDS (1 wt%), the E_{22} vs. E_{11} plots shifted to the positions indicated by the red stars in Fig. 6. The plots of these SWNTs are almost identical to those obtained for the SWNTs wrapped with SDS by using O'Connell's method, as mentioned in section 2.4, which implies that the free-standing SWNTs were wrapped with SDS by immersing them in the SDS solution.
Most E_{11} and E_{22} of SDS-wrapped SWNTs exhibit redshifts as compared to the free-standing SWNTs in air, except for E_{22} of near-zigzag Type II SWNTs, which exhibit blueshifts. (Ohno, Iwasaki et al. 2006) This behavior is different from the results obtained for the dependence of E_{11} and E_{22} on the dielectric constant of the surrounding material, as described above, in which all E_{11} and E_{22} exhibited redshifts with an increase in the dielectric constant. The positions of the E_{22} vs. E_{11} plots of the SDS-wrapped SWNTs shift so that the $(2n + m)$-family pattern spreads more widely, in addition to the shift due to the dielectric screening effect. This behavior of the energy shifts is similar to stress-induced shift. (Arnold, Lebedkin et al. 2004) One plausible explanation for the effect of SDS wrapping is that the SWNT is compressed by the surfactant molecules in the radial direction, resulting in the uniaxial strain that modifies the bandgap of the SWNT.

3.4 Effect of substrate

Even though a substrate is one of the indispensable parts for device application of SWNTs and supports the SWNTs and electrodes, the contact of SWNTs with the substrate seriously affects the optical properties of SWNTs. For example, in the case of SWNTs grown on a substrate such as SiO_2, PL is strongly suppressed if the body of the SWNT lies on the substrate. (Ohno, Kishimoto et al. 2006) The quenching of PL suggests that the excitons excited in an SWNT recombine by a nonradiative recombination process, probably via interface states between the SWNT and the substrate. The interface states also cause serious degradation of not only the optical properties but also the electrical properties of SWNTs, for example, the capture and emission of carriers at the interface states may cause noise in SWNT FETs.(Lin, Tsang et al. 2007)
Even though PL spectroscopy is not applicable to such SWNTs directly grown on a substrate, photocurrent spectroscopy is useful to study the optical properties of such SWNTs.(Ohno, Kishimoto et al. 2004) Figure 8 shows the photocurrent spectra of two types of transistors; one transistor is a conventional SWNT transistor with a channel lying on a SiO_2/Si substrate, and the other is a transistor with a channel of a free-standing SWNT, as shown in the inset. The peaks in the spectra are attributed to E_{22} of the semiconducting SWNT. In the case of the free-standing SWNT, the peak is quite sharp and has an FWHM of 30 meV, which is

comparable to the excitation spectrum of the PL of an SWNT. On the other hand, in the case of the SWNT lying on SiO_2, the peak structure is not clear, and the FWHM is as broad as 60 meV. The broadening of the spectrum suggests that the energy band of this SWNT is modified inhomogeneously, probably depending on the surface structure of amorphous SiO_2.

Recently, Xie et al. have reported that PL can be observed from SWNTs lying on a SiO_2 surface when the SWNTs are transferred to another substrate after the growth. (Xie, Liu et al. 2007) At room temperature, it is difficult to form interface states between an SWNT and a SiO_2 substrate; this is because both the SWNT and SiO_2 are chemically stable. Nevertheless, during the growth of SWNTs directly on a substrate, chemical bonds may be formed at the interface due to high growth temperature. Such chemical bonds may act as nonradiative recombination centers. Moreover, Xie et al. have also reported that the PL was enhanced when the substrate surface was covered with a self-assembled monolayer. It has been explained on the basis of carrier transfer to the traps present in the SiO_2 layer of the substrate.

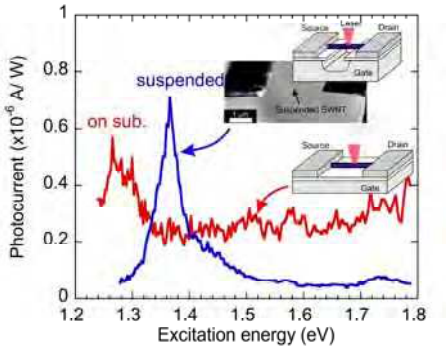

Fig. 8. Photocurrent spectra of CNTFETs with a free-standing SWNT (blue) and a SWNT in contact with a substrate (red).

4. Summary

In this chapter, we discussed environmental effects on the optical properties of SWNTs. Detailed understandings of the environmental effects help us to make a spectroscopic technique a standardized methodology to evaluate the chirality abundance and the quality of SWNTs. It is also interesting to develop sensing tools of nano dimensions for bio and medical applications by utilizing the environmental effects.

Acknowledgments

The authors thank S. Iwasaki, A. Kobayashi, Y. Murakami, Y. Miyauchi, and R. Saito for fruitful collaborations and discussions. This study is partially supported by Grant-in-Aid from MEXT, Japan.

5. References

Ando, T. (2005). "Theory of electronic states and transport in carbon nanotubes." Journal of the Physical Society of Japan **74**(3): 777-817.

Arnold, K., S. Lebedkin, et al. (2004). "Matrix-imposed stress-induced shifts in the photoluminescence of single-walled carbon nanotubes at low temperatures." Nano Letters **4**(12): 2349-2354.

Bachilo, S. M., M. S. Strano, et al. (2002). "Structure-assigned optical spectra of single-walled carbon nanotubes." Science **298**(5602): 2361-2366.

Chiashi, S., S. Watanabe, et al. (2008). "Influence of Gas Adsorption on Optical Transition Energies of Single-Walled Carbon Nanotubes." Nano Letters **8**(10): 3097-3101.

Chou, S. G., H. B. Ribeiro, et al. (2004). "Optical characterization of DNA-wrapped carbon nanotube hybrids." Chemical Physics Letters **397**(4-6): 296-301.

Duesberg, G. S., I. Loa, et al. (2000). "Polarized Raman spectroscopy on isolated single-wall carbon nanotubes." Physical Review Letters **85**(25): 5436-5439.

Fantini, C., A. Jorio, et al. (2004). "Optical transition energies for carbon nanotubes from resonant Raman spectroscopy: Environment and temperature effects." Physical Review Letters **93**(14): 147406.

Finnie, P., Y. Homma, et al. (2005). "Band-gap shift transition in the photoluminescence of single-walled carbon nanotubes." Physical Review Letters **94**(24): 247401.

Hagen, A., G. Moos, et al. (2004). "Electronic structure and dynamics of optically excited single-wall carbon nanotubes." Applied Physics a-Materials Science & Processing **78**(8): 1137-1145.

Hertel, T., A. Hagen, et al. (2005). "Spectroscopy of single- and double-wall carbon nanotubes in different environments." Nano Letters **5**(3): 511-514.

Hirori, H., K. Matsuda, et al. (2006). "Exciton localization of single-walled carbon nanotubes revealed by femtosecond excitation correlation spectroscopy." Physical Review Letters **97**(25): 257401.

Ichida, M., Y. Hamanaka, et al. (2002). "Ultrafast relaxation dynamics of photoexcited states in semiconducting single-walled carbon nanotubes." Physica B-Condensed Matter **323**(1-4): 237-238.

Iwasaki, S., Y. Ohno, et al. (2007). "Environmental dielectric screening effect on exciton transition energies in single-walled carbon nanotubes." arXiv:0704.1018v1 [cond-mat.mtrl-sci].

Jorio, A., C. Fantini, et al. (2005). "Resonance Raman spectroscopy (n,m)-dependent effects in small-diameter single-wall carbon nanotubes." Physical Review B **71**(7): 075401.

Kataura, H., Y. Kumazawa, et al. (1999). "Optical properties of single-wall carbon nanotubes." Synthetic Metals **103**(1-3): 2555-2558.

Lefebvre, J., D. G. Austing, et al. (2006). "Photoluminescence imaging of suspended single-walled carbon nanotubes." Nano Letters **6**(8): 1603-1608.

Lefebvre, J., J. M. Fraser, et al. (2004). "Photoluminescence from single-walled carbon nanotubes: a comparison between suspended and micelle-encapsulated nanotubes." Applied Physics a-Materials Science & Processing **78**(8): 1107-1110.

Lin, Y. M., J. C. Tsang, et al. (2007). "Impact of oxide substrate on electrical and optical properties of carbon nanotube devices." Nanotechnology **18**(29): 295202.

Miyauchi, Y., R. Saito, et al. (2007). "Dependence of exciton transition energy of single-walled carbon nanotubes on surrounding dielectric materials." Chemical Physics Letters **442**(4-6): 394-399.

Miyauchi, Y. H., S. H. Chiashi, et al. (2004). "Fluorescence spectroscopy of single-walled carbon nanotubes synthesized from alcohol." Chemical Physics Letters **387**(1-3): 198-203.

Moore, V. C., M. S. Strano, et al. (2003). "Individually suspended single-walled carbon nanotubes in various surfactants." Nano Letters **3**(10): 1379-1382.

Nosho, Y., Y. Ohno, et al. (2007). "The effects of chemical doping with F(4)TCNQ in carbon nanotube field-effect transistors studied by the transmission-line-model technique." Nanotechnology **18**(41): 415202.

O'Connell, M. J., S. M. Bachilo, et al. (2002). "Band gap fluorescence from individual single-walled carbon nanotubes." Science **297**(5581): 593-596.

Ohno, Y., S. Iwasaki, et al. (2006). "Chirality-dependent environmental effects in photoluminescence of single-walled carbon nanotubes." Physical Review B **73**(23): 235427.

Ohno, Y., S. Iwasaki, et al. (2007). "Excitonic transition energies in single-walled carbon nanotubes: Dependence on environmental dielectric constant." Physica Status Solidi B-Basic Solid State Physics **244**(11): 4002-4005.

Ohno, Y., S. Kishimoto, et al. (2006). Carrier transport property in single-walled carbon nanotubes studied by photoluminescence spectroscopy. Journal of Physics: Conference Series. **38:** 5-8.

Ohno, Y., S. Kishimoto, et al. (2006). "Photoluminescence of single-walled carbon nanotubes in field-effect transistors." Nanotechnology **17**(2): 549-555.

Ohno, Y., S. Kishimoto, et al. (2004). "Chirality assignment of individual single-walled carbon nanotubes in carbon nanotube field-effect transistors by micro-photocurrent spectroscopy." Applied Physics Letters **84**(8): 1368-1370.

Okazaki, T., T. Saito, et al. (2006). "Photoluminescence and population analysis of single-walled carbon nanotubes produced by CVD and pulsed-laser vaporization methods." Chemical Physics Letters **420**(4-6): 286-290.

Ostojic, G. N., S. Zaric, et al. (2004). "Interband recombination dynamics in resonantly excited single-walled carbon nanotubes." Physical Review Letters **92**(11): 117402.

Oyama, Y., R. Saito, et al. (2006). "Photoluminescence intensity of single-wall carbon nanotubes." Carbon **44**(5): 873-879.

Perebeinos, V. and P. Avouris (2008). "Phonon and electronic nonradiative decay mechanisms of excitons in carbon nanotubes." Physical Review Letters **101**(5): 057401.

Perebeinos, V., J. Tersoff, et al. (2004). "Scaling of excitons in carbon nanotubes." Physical Review Letters **92**(25): 257402.

Saito, R., G. Dresselhaus, et al. (1998). Physical Properties of Carbon Nanotubes. Singapore, World Scientific Publishing Co. Pte. Ltd.

Saito, R., G. Dresselhaus, et al. (2000). "Trigonal warping effect of carbon nanotubes." Physical Review B **61**(4): 2981-2990.

Spataru, C. D., S. Ismail-Beigi, et al. (2005). "Theory and ab initio calculation of radiative lifetime of excitons in semiconducting carbon nanotubes." Physical Review Letters **95**(24): 247402.

Wang, F., G. Dukovic, et al. (2004). "Time-resolved fluorescence of carbon nanotubes and its implication for radiative lifetimes." Physical Review Letters **92**(17): 177401.

Wang, F., G. Dukovic, et al. (2005). "The optical resonances in carbon nanotubes arise from excitons." Science **308**(5723): 838-841.

Xie, L. M., C. Liu, et al. (2007). "Photoluminescence recovery from single-walled carbon nanotubes on substrates." Journal of the American Chemical Society **129**(41): 12382.

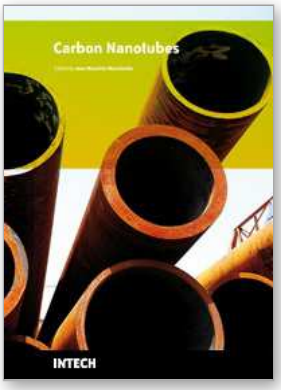

Carbon Nanotubes

Edited by Jose Mauricio Marulanda

ISBN 978-953-307-054-4
Hard cover, 766 pages
Publisher InTech
Published online 01, March, 2010
Published in print edition March, 2010

This book has been outlined as follows: A review on the literature and increasing research interests in the field of carbon nanotubes. Fabrication techniques followed by an analysis on the physical properties of carbon nanotubes. The device physics of implemented carbon nanotubes applications along with proposed models in an effort to describe their behavior in circuits and interconnects. And ultimately, the book pursues a significant amount of work in applications of carbon nanotubes in sensors, nanoparticles and nanostructures, and biotechnology. Readers of this book should have a strong background on physical electronics and semiconductor device physics. Philanthropists and readers with strong background in quantum transport physics and semiconductors materials could definitely benefit from the results presented in the chapters of this book. Especially, those with research interests in the areas of nanoparticles and nanotechnology.

INTECH
open science | open minds

InTech Europe
University Campus STeP Ri
Slavka Krautzeka 83/A
51000 Rijeka, Croatia
Phone: +385 (51) 770 447
Fax: +385 (51) 686 166
www.intechopen.com

InTech China
Unit 405, Office Block, Hotel Equatorial Shanghai
No.65, Yan An Road (West), Shanghai, 200040, China
中国上海市延安西路65号上海国际贵都大饭店办公楼405单元
Phone: +86-21-62489820
Fax: +86-21-62489821